SIMULATION OF THE COMPRESSION MOLDING OF UNIDIRECTIONAL COMPOSITE LEAF SPRINGS

B. Gardarein [1], P. Durand[2], P. Lory [1]
[1] *Research Department, RENAULT*
[2] *Materials Engineering Department, RENAULT*
Technocentre RENAULT, TCR RUC 429, 1 Av. du Golf , 78288 Guyancourt Cedex, France

SUMMARY: The aim of this paper is to introduce the software LAME2D, developed by RENAULT Research Department, to simulate the compression molding process of composite leaf springs. The theoretical model is detailed, and the performances of the software are discussed using as a representative example a particular leaf spring shape. Several moulding conditions are examined, i.e. the height of the spring, the punch velocity, ad the tool temperature. The simulation results are compared with instrumented experiments, and it is shown that in each case, the model is able to predict with reasonable accuracy the temperature evolution and the fibre distribution in every location of the spring, which makes it an useful and reliable tool for the optimisation of the process.

KEYWORDS: compression moulding, simulation, unidirectional prepregs

INTRODUCTION

RENAULT used to produce composite leaf springs dedicated to light commercial vehicles like TRAFIC and MASTER. A software named LAME2D was developed to simulate the compression molding process and to optimize the forming parameters. The aim of the simulation is namely to reduce the cycle time and hence the development cost of the springs by controlling the chemorheological state of the composite material all along the process.
In this paper, we will explain the way the process was analyzed and decomposed, which will lead us to the mathematical description of the model. Then, we will illustrate the performances of the simulation, using the example of a prototype spring.

PROCESS ANALYSIS

The forming process consists, first, in piling up several layers of fibre/resin prepregs to prepare a preform of the spring. The layers may not have the same length, which will induce the variable height of the spring (see fig. 1). The knowledge of the exact composition of the prepregs and of the morphology of the preform is essential, as we will show it determines the final mean composition of the spring.
Next, the preform is laid in a hot mould, and the compression moulding process begins. Using a batch of experiments first performed on plates, it was decomposed in four main steps, analysed below for sample plates.

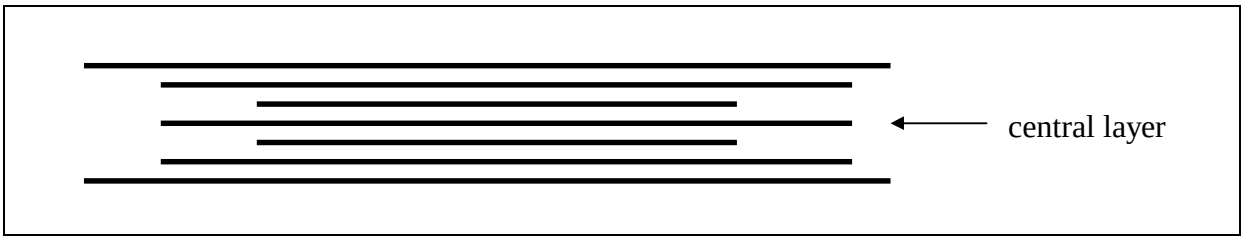

Fig. 1: Flat scheme of a 7 layer preform

Pre-heating of the shape

As the punch comes down to reach the surface of the preform, the heat of the die diffuses in the preform. The temperature of the spring begins to rise rapidly at the lower surface of the preform, which induces an almost immediate cure of the external layers, and more slowly in the internal layers, in which the resin begins to melt. At this stage, no resin extraction and no preform movement have been detected. The main physical phenomena are the heat conduction between the lower die and the preform, and the resin melting and cure. As the move of the punch towards the lower die is fast enough, we were allowed to neglect the heat exchanged by radiation between the punch and the top surface of the preform.

Lateral motion of the preform

That step begins when the punch reaches the top surface of the preform. In most cases, the preform width is about 10mm less than the die's, which makes it easier for the operator to lay the preform down in the mould. Thus, the melt preform has first the ability to fill the die by a lateral motion. No resin extraction has been registered yet, but most of the air trapped in the preform during the piling up of the layers is evacuated. The height and width of the preform change.

Resin extraction

The die is now filled with a preform composed almost exclusively of fibres and resin. Finer observations shows that residual air bubbles could stay entrapped within the layers, but they do not represent a significant volume ratio to be quantified, and thus the presence of air has been neglected. As the punch is still moving downward and there is no place left in the mould, the only way for the preform to adjust its volume is to eject the melted resin out of the die. Firing measurements on interrupted shots have shown that the resin seems to flow along the longitudinal direction of the fibres. The displacement imposed on the punch is stopped when the final shape of the part has been reached.

Cure

The punch is maintained in its final position by applying an hydraulic pressure. The part remains motionless within the mould until the complete solidification of the resin is achieved. The cure of the resin induces an exothermic reaction, which in general occurs at this stage of the process, and needs to be controlled to avoid the resin degradation.

Adaptation of the scenario to variable height spring shapes

This decomposition of the process has been examined on several spring shapes, and appeared to be still valid, if it is applied separately on the different sections of the preform. A section is a short cut of the preform which global height and width can be considered uniform during the process (see fig. 2).

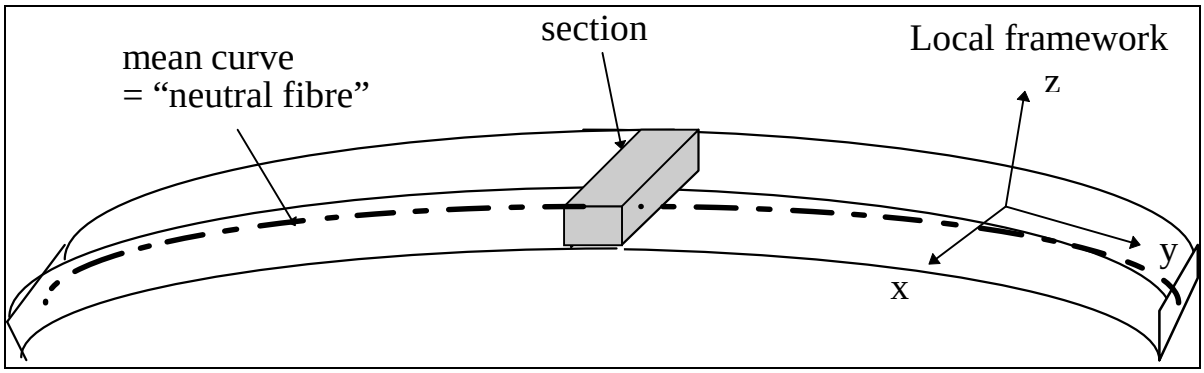

Fig. 2 : General aspect of a variable height leaf spring

It was observed and can easily be demonstrated that, for a spring shape with variable height, the punch comes into contact gradually with the top surface of the preform, which means one section after another. Hence, the lateral motion of a section may not end at the same instant as the lateral motion of its neighbours.
Additionally, the resin fluxes travelling between the different sections have to be considered in the model, as they induce extra heat and cure exchanges (« convected fluxes »).
Finally, provided that we take care of applying the appropriate scenarii and of carrying the correct amount of resin from one section to another, it has been shown that an isolated section behave just like a plate.

MODEL DESCRIPTION

Main hypotheses

General hypotheses: The compression is simulated using a 2D model, defined on a longitudinal section of the spring. The temperature and fibre volume fraction measurements performed all along the process on different locations of the springs have assessed the validity of our hypothesis.
The air pockets trapped in the preform is supposed to be extracted during the lateral motion of the spring. This is not entirely true, but the remaining air bubbles are too fine to be quantified.
Flow model hypotheses: One of the most important hypothesis of the model is that, due to the high ratio L/h of the spring, the pressure remains constant across the height h of the spring.
Moreover, it is supposed that the molten resin flows mainly along the longitudinal direction of the fibres. This results from the moulding conditions: during the resin extraction step, there is no lateral movement of the spring in the die, and it has been shown, for example in the RTM process, that the resin follows the easiest way leading to the exit of the die, which excludes exchanges between the layers. Such transversal fluxes would also violate the assumption of constant pressure throughout the height of the spring.
Heat model hypotheses: Due to the L/h ratio of the spring, the heat diffusion is supposed 1D along the height of the spring.
Due to the hypotheses on the movement of the resin, the convected fluxes may also be supposed 1D along the longitudinal direction of the spring.

Heat model

Each elementary volume of the spring is submitted to the energy equation of thermosets, which we decided to express on the composite, because it leads to an easier material characterisation :

$$\rho C_p \frac{\partial T}{\partial t} + \rho_r C_{pr} \vec{v}.\vec{\nabla}T = \vec{\nabla}\left(\lambda \vec{\nabla}T\right) + S_{exo} \qquad (1)$$

In the first left hand term, representing the temperature variation of the elementary volume, T is the temperature of the composite, ρ and C_p are respectively the density and specific heat of the composite. In the second left-hand term of the equation, which results from the resin flux across the volume, C_{pr} is the specific heat of the resin, and $\vec{v}$ is the resin velocity. In the right hand terms, λ is the conductivity of the composite and S_{exo} is the heat source resulting from the exothermic cure of the resin :

$$S_{exo} = (1 - t_{vv})\rho_r \dot{\alpha} \Delta H_t^r \tag{2}$$

where t_{vv} is the fibre volume fraction in the composite, ρ_r is the resin density, $\dot{\alpha}$ is the resin cure rate, and ΔH_t^r is the heat mass transfer of the resin during the cure reaction.

The boundary conditions are an imposed temperature T_{surf}^{die} at the surface of the die, and a Fourier diffusion condition between the die and the surface of the spring :

$$\left[T_{surf}^{spring} - T_{surf}^{die}\right] = R_c\left(\lambda \frac{\partial T}{\partial n}\right) \tag{3}$$

where R_c is the contact resistance of the die.
At the ends of the spring, and at the top surface of the spring during the pre-heating step of the process, no heat flux is allowed :

$$\frac{\partial T}{\partial n} = 0 \tag{4}$$

The initial temperature of the preform is taken equal to the room temperature.

Cure kinetics

The degree of cure is calculated from the following equation, which includes the cure kinetics itself, but also a transport term resulting from the resin flux through the elementary volume :

$$\frac{\partial \alpha}{\partial t} + (1 - t_{vv})\vec{v}.\vec{\nabla}\alpha = \dot{\alpha}(T, \alpha) \tag{5}$$

The expression of the cure rate $\dot{\alpha}(T, \alpha)$ depends on the nature of the resin and is determined from Differential Scanning Calorimetry (DSC) measurements.

Flow model

Evolution of the spring geometry

During the two steps preceding the resin extraction, the composition of the elementary volumes does not change, and the significant values we have to determine are :

- the contact between the punch and the top surface of the considered section of the spring,
- the end of the lateral motion of the section,
- the evolution of the height and fibre volume fraction of the section, as soon as the contact with the punch has occurred.

These values are calculated from the initial preform characteristics and from the actual position p of the punch :

$$p = e_f + \delta h \cos(\alpha) \tag{6}$$

where e_f is the final height of the section, δh is the actual distance between the punch and this final height (known directly from the moulding cycle), and α is an angle representing the curvature of the section (see fig. 3).
The instant of contact is determined from the comparison of the actual punch position p and the initial height of the section e_0 :

$$e_0 = N_f < e_{ply} >= \frac{N_f N_m m_{lv}}{L_i \rho_v t_{vv}^0} \tag{7}$$

where N_f is the number of plies in the section, and $<e_{ply}>$ is the mean height of a ply. That mean height is calculated from the characteristics of the ply, which are the number of rovings

in a ply N_m, the specific weight of a roving m_{lv}, the initial width L_i of the ply the density of the fibre ρ_v, and the initial fibre volume fraction in the plies t_{vv}^0, given by Eqn 8.

$$t_{vv}^0 = \frac{\rho_r \left(1 - t_{mr}^0\right)}{\rho_v t_{mr}^0 + \rho_r \left(1 - t_{mr}^0\right)} \tag{8}$$

where t_{mr}^0 is the initial resin weight ratio.

The end of the lateral motion of the section, which coincides with the beginning of the resin extraction from the section, is known from the comparison of the width of the die Lf and the actual width of the section, which leads to Eqn 9 :

$$e_f + \delta h.\cos(\alpha) = e_0 \frac{L_i}{L_f} \tag{9}$$

Note that a section belonging to the pre-heating or lateral motion steps may receive a flux of resin from the neighbour sections in which the resin extraction step has begun, and thus the fibre volume fraction has to be actualised in each elementary volume of the section (see Eqns 14, 15).

Resin extraction

The resin extraction model is based on the assumption of constant pressure P through the height of a section ($\frac{\partial P}{\partial z} = 0$) and on Darcy's law :

$$\vec{v} = -\frac{\overline{\overline{K}}}{\eta}.\vec{\nabla}P \tag{10}$$

where $\vec{v}$ is the velocity of the resin, η is its viscosity, and $\overline{\overline{K}}$ is the permeability tensor of the fiber network, in which we suppose that only the longitudinal permeability of the unidirectional network K_{yy}, expressed in the local reference framework (y,z) of our spring section, is significant for our model.

The main pressure equation applied on each section (Eqns 13a and 13b) is obtained from combining the resin incompressibility :

$$\vec{\nabla}.\vec{v} = 0 \tag{11}$$

and Darcy's law, applied on each elementary volume $d\Omega$, Ω being the total volume of the spring :

$$\int_{\Omega} \vec{\nabla}.\left(\frac{\overline{\overline{K}}}{\eta}.\vec{\nabla}P\right) d\Omega = 0 \tag{12}$$

Assuming that the pressure applied on the section remains negligible (P=0) until resin extraction step has begun, and knowing that the punch moves with an imposed velocity $\dot{h}$, we finally obtain :

$$\frac{\partial}{\partial y}\left(\overline{S}\frac{\partial P}{\partial y}\right) = \dot{h} \tag{13a}$$

where

$$\overline{S} = \int_0^{h(y)} \frac{K_{yy}}{\eta} dz \tag{13b}$$

Actualisation of the local fibre volume fraction

The local volume fraction is calculated from Darcy's law (Eqn 10), which gives the resin flux in each elementary volume ω of the section for a time interval δt. The elementary volume variation is thus known :

$$\delta\omega = \delta t . \int_{\partial\omega} S_\omega \frac{\partial P(y)}{\partial y} d(\partial\omega) \qquad \text{where} \qquad S_\omega = -\frac{K_{yy}}{\eta}\bigg|_\omega \tag{14}$$

The fibre volume fraction is calculated from dω and the volume of fibres ω_v present in the elementary volume ω :

$$t_{vv} = \frac{\omega_v}{\omega - \delta\omega} \tag{15}$$

Material behaviour

The characterisation of the composite behaviour during the moulding process was performed using both classical measurement protocols and instrumented plates together with the model itself.

Some data, like some resin intrinsic characteristics (cure kinetics, viscosity, specific heat), and the permeability of the fibre network were accessible from classical means (respectively DSC, rheometry, calorimetry, standard permeability measurements), but the characterisation of the composite conductivity and specific heat required instrumented plates and the use of our software as an inverse characterisation tool.

As the material behaviour depends on the resin and fibre used in the process, we will only record here the main dependencies we had to take into account for each composite characteristic (see Table 1), and the way intrinsic resin and fibre characteristics were homogenised to obtain the composite characteristics.

Unknowns of the model	Temperature T	Degree of cure α	Fibre volume fraction t_{vv}
Composite density ρ			x
Composite specific heat C_p	x	x	x
Composite conductivity λ		(x)	x
Resin viscosity η	x	x	
Fibre network longitudinal permeability K_{yy}			x

Table 1 : Main dependencies of the material characteristics

Finally, we used the following homogenisation laws for the composite characteristics :

Density :
$$\rho = t_{vv}\rho_v + (1 - t_{vv})\rho_r \tag{16}$$

Specific heat :
$$C_p(t_{vv}, T, \alpha) = \frac{t_{vv}\rho_v C_{pv}(T) + (1 - t_{vv})\rho_r C_{pr}(T, \alpha)}{t_{vv}\rho_v + (1 - t_{vv})\rho_r} \tag{17}$$

Conductivity :
$$\lambda(t_{vv}) = \lambda_r \left(\frac{(1 + t_{vv})\lambda_v + (1 - t_{vv})\lambda_r}{(1 - t_{vv})\lambda_v + (1 + t_{vv})\lambda_r} \right) \tag{18}$$

We observed that the resin conductivity λ_r may depend on the degree of cure, but this dependency happened to be very light. Thus, we estimated it was not useful to take it into account in most cases.
The way the resin chemorheological characteristics may depend on temperature and degree of cure has been extensively described in a recent review [1]. There are also several references expressing the longitudinal permeability of an unidirectional fibre bed either with a Kozeny-Carman expression [2, 3, 4], which is the most frequently used and proved to be sufficient in our case (see Eqn 19), or with more complicated expressions [5, 6].

$$K_{yy}(t_{vv}) = K_0 \frac{(1 - t_{vv})^3}{t_{vv}^2} \tag{19}$$

K0 is a characteristic value of the fibre bed.

Numerical analysis

The spring were discretized using the cross-sections definition along the longitudinal direction of the spring, and a constant number of representative volume per cross-section in the transversal (height) direction of the part. A constant number of mesh layers does not mean a constant number of real prepreg plies towards the spring, but the assumption of a constant height discretization is only possible when the spring shows a very slow variation of the number of prepregs along the longitudinal direction of the part. The resulting elements are not rigorously contiguous, but the volume value itself is the exact one (see fig. 3).
We used a finite volume / finite difference analysis, so that each element of the mesh is associated to a representative volume (or cell), towards which all fluxes (heat, resin, degree of cure) are evaluated with the classical balance equations.

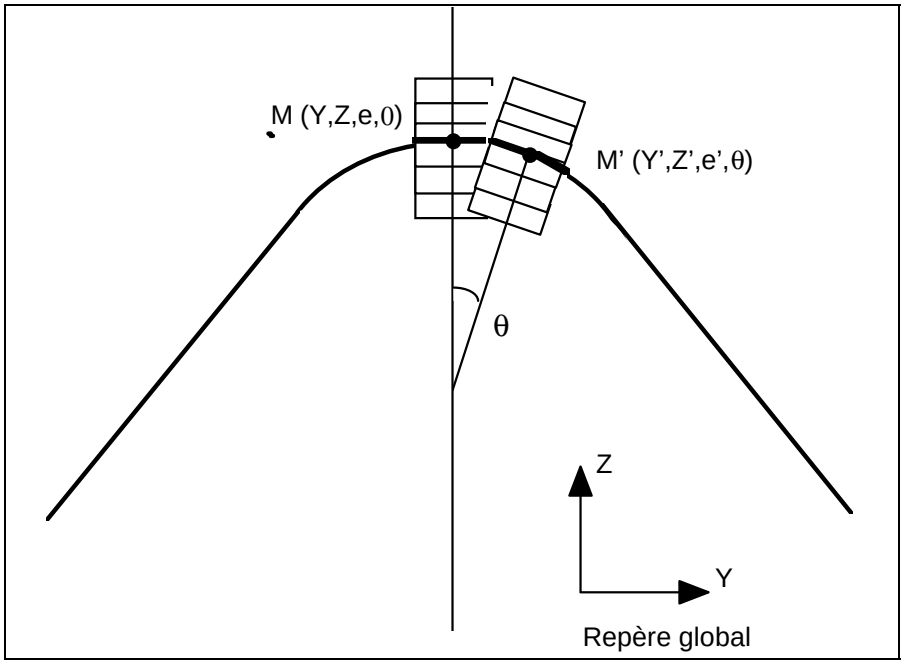

Fig. 3 : Scheme of the spring discretization

PROCESS ANALYSIS FOR A PROTOTYPE LEAF SPRING

Basic processing principles

We performed process optimisation on many sample plates of different height, and for two different types of prepregs. We also examined several leaf spring shapes and compared the predictions of the model with temperature and fibre volume fraction measurements. In the following, we will detail the results obtained for a peculiar spring shape.

But first of all, let us state some basic principles, which make it easier to understand the part behaviour during the moulding process. To make the demonstration easier ,let us assume the part is a plate, or a specific section in a spring.

Influence of the punch velocity : It has been demonstrated that for a given temperature imposed to the die, the faster the punch moves, the higher the fibre volume fraction in the intermediate layers of the plate. Inversely, the slower the punch moves, the higher the fibre volume fraction in the core layers of the plate. This is due to the competition between heat diffusion in the plate and resin melting and cure. The external layers are in contact with the hot dies and solidify quasi instantaneously. For a fast movement of the punch, the heat has just time to propagate to the intermediate layers, and the core layers are still cold. Thus, the core resin is still not melted and hence unable to flow. For a slow movement of the punch, the core layers may be melted, but the resin cure begins in the intermediate layers and solidification may occur too early in those layers.

Influence of the tool temperature : The influence of the temperature in the dies is less important than the velocity of the punch, provided that this temperature is high enough to give the composite the heat necessary to melt and then cure rapidly the amount of resin present in the preform. The higher the temperature, the higher the fibre volume fraction gradient near the surface of the plate, and the higher the risk of overheating the composite by the means of an uncontrolled exotherm. On the contrary, the lower the temperature, the slower the time cycle.

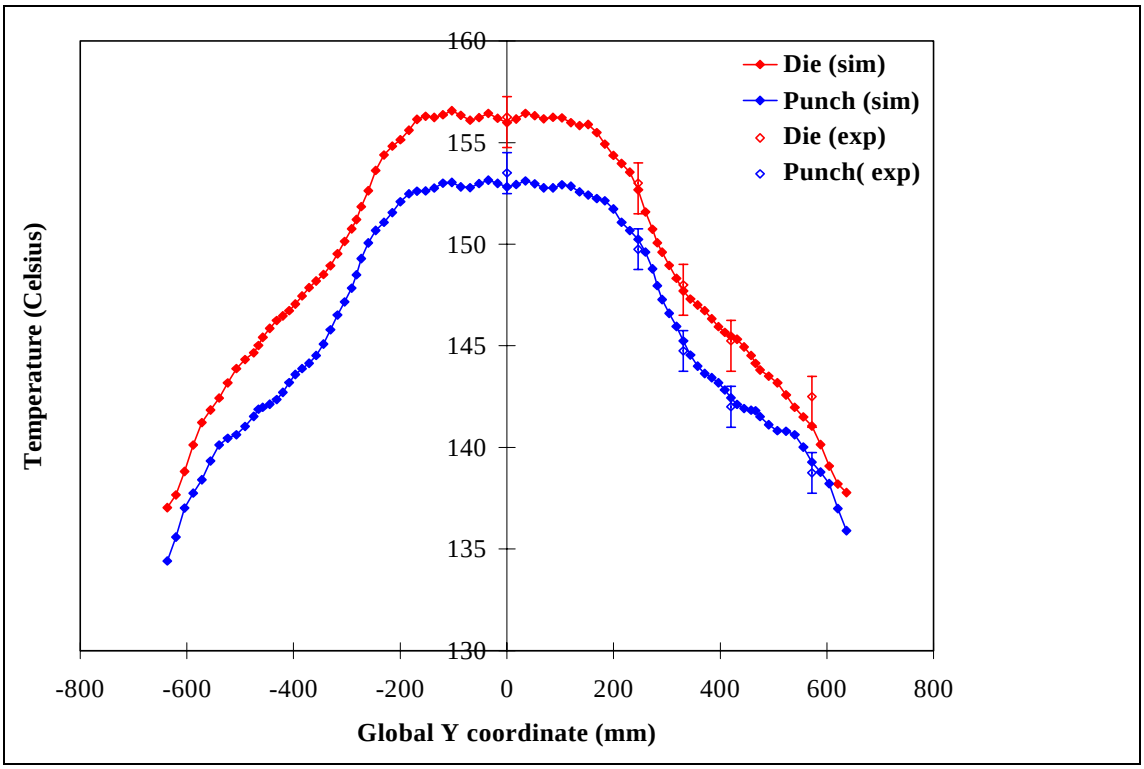

Fig. 4 : Correlation of measured and simulated tool temperature profiles

Heat regulation of the tools : For the plate moulds, the problem of the heat regulation is quite simple, as the temperature at the surface of each die is regulated to be homogeneous on the die surface. But for the spring shapes, the temperature imposed to the die may vary significantly along the longitudinal axis of the spring. Moreover, the temperature of the die being regulated by an hydraulic system, we only know the input/output temperatures, and not the temperature profile on the surface of the die. We demonstrated that the experimental profile could be reached by calculating the 3D heat transfers between the regulation system and the die. We calculated the temperature profiles at the surface of the dies with the 3D model CLIP-TO [7].
Fig. 4 shows there is a quite good correlation between the calculated and measured temperature profiles at the surface of the punch and of the die. The problem is that the 3D calculation requests the meshing of the whole hydraulic system, and a sufficient knowledge of the thermal and flow parameters. Unfortunately, we also demonstrated that this calculation could not be simplified enough to be introduced easily in our model. Thus, the impossibility to predict the tool temperature profiles remains the weak point of the LAME2D software.

Data for the simulation of the moulding process

The data requested for the simulation are :

- a geometric file giving, for each section of the spring, the global coordinates of the « neutral fibre », the angle of curvature a, the final height and width of the spring e_f and L_f, and the number of plies N_f in the section,
- the material characteristics (see Table 1), including the ply composition,
- the cycle characteristics, i.e. the successive positions of the punch, and the temperatures at the surface of the upper and lower tool for each section of the spring,
- a file specifying the required outputs.

From a basic spring shape and moulding conditions, we extrapolated variations of spring height, punch velocity and tool temperature profiles, recorded in Table 2.

Simulation code	Spring maximum height (mm)	Punch velocity (type)	Centre / ends temperature (°C) (centre = central section)	Figures
R (reference)	14.77	slow	157 / 148	5
A	20	slow	157 / 148	6, 7
B	14.77	fast	157 / 148	6
C	14.77	slow	147 / 138	6

Table 2 : Selected processing conditions for the prototype spring

For each set of moulding conditions, we realised a batch of three or more instrumented experiments, in which we measured the temperature along the moulding process, and the final fibre volume fraction at different locations in the spring. We will show in the next paragraphs that in each case, the software provides a quite good prediction of the temperature and composition profiles.
Each calculation is lasting about 100 CPUs on a Silicon Graphics Octane R10000.

Confrontation of the simulation and experimental results

The results obtained reference case is illustrated on Fig. 5. The evolution of temperature calculated at the centre and at the right end of the spring on bottom and top layers are compared with the corresponding die and punch thermocouple outputs. It is shown that, excepted for the beginning of the process, the accuracy of the temperature prediction is 5°C and about 50s, which corresponds to the reproductiveness of the experiments. The important discrepancies observed during the first time steps, which we did not occur in plates, were

related to a rough contact between the preform and the lower tool. The length and curvature of the spring makes it difficult for the operator to lay it accurately on the die. This leads to random temperature evolution, which the software is of course not able to predict. Fortunately, as soon as the punch has come into contact with the preform, the contact with the die is established, and the simulation happens to be predictive again.

The influence of the moulding conditions on the temperature evolution in the die is illustrated on Fig. 6 through the centre-core temperature curves of cases A, Band C. The model accuracy is somewhat lower in case B, as a difference of 12°C on the exotherm is recorded, but the prediction is still acceptable, according to the dispersion observed on the experimental results. The relative positions of the core temperature curves is coherent with the basic principles explained above : a slower punch velocity leads to a late core exotherm, and a lower tool temperature leads to a slightly lower exotherm.

It is also interesting to evaluate the influence of the moulding conditions on the fibre distribution in the spring. Fig. 7 shows the simulated and experimental final distributions taken at the intermediate and end sections of spring A. The maximum absolute discrepancy of the simulation is of about 2%vol., which is equal to the precision of the measurement. The brutal variations in fibre volume distribution have to be taken carefully. They apparently result from the assumption of no transversal fluxes. Between the sections containing a different number of layers, the resin fluxes are not evenly redistributed, as it would be in reality. The only way to reduce this phenomenon would be to develop a more complex model, which would be more precise, but also more expensive in time.

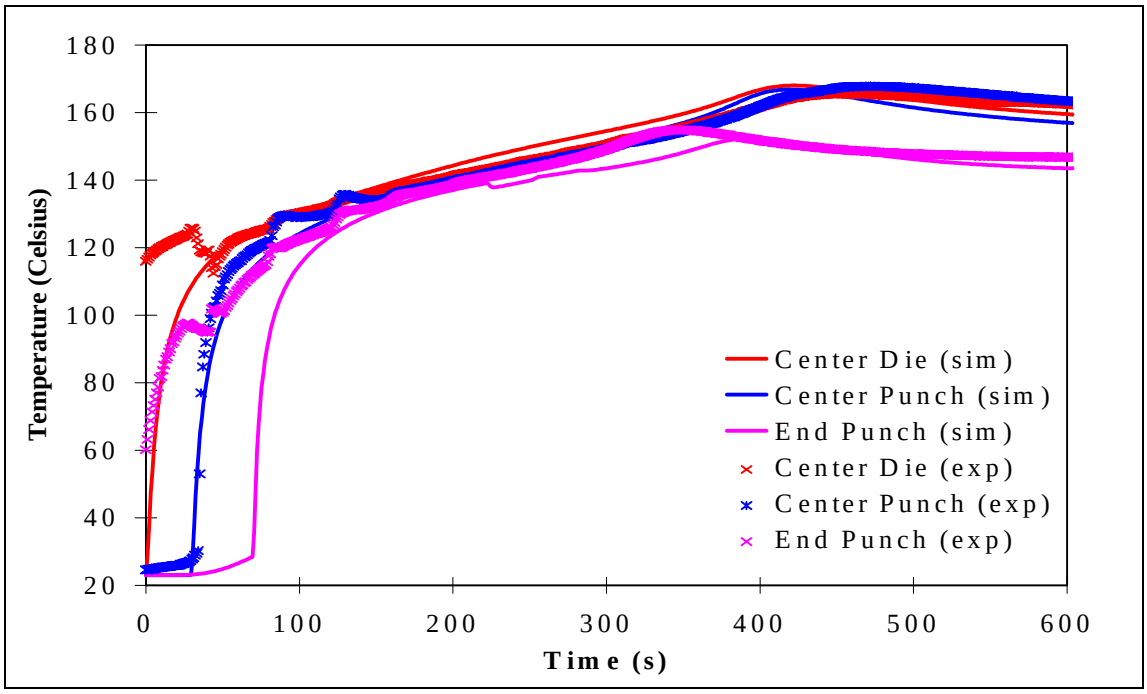

Fig.5 : Temperature curves for case R

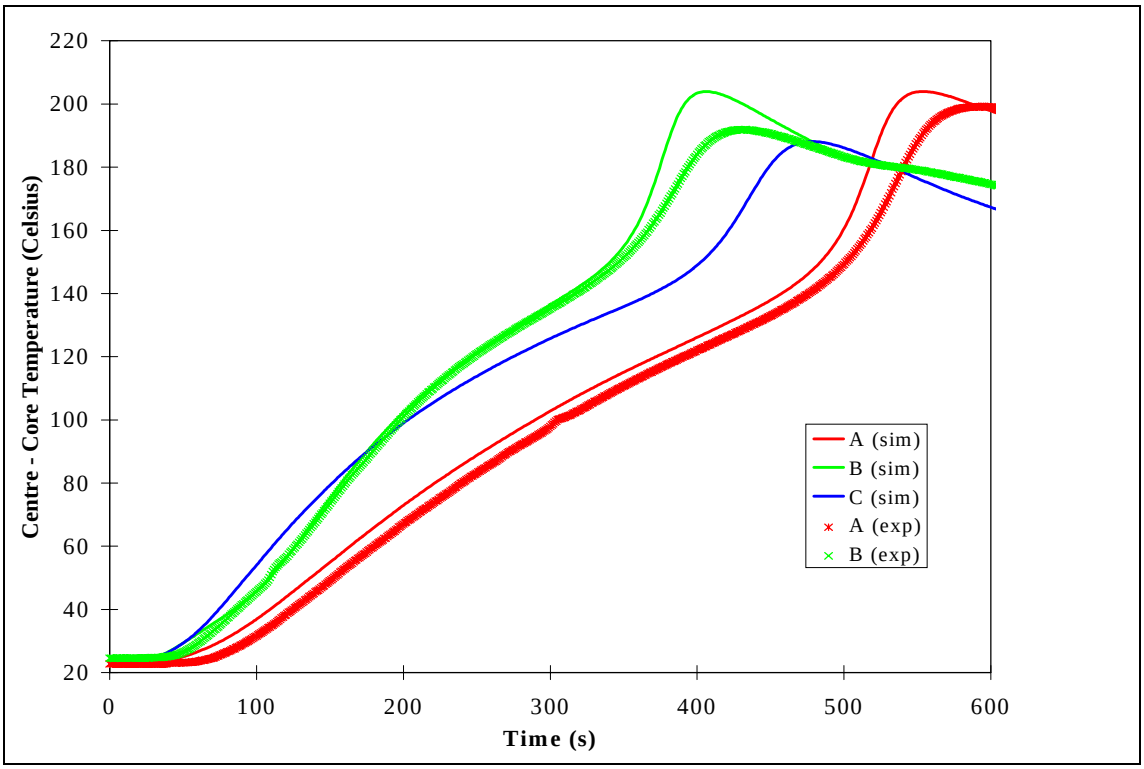

Fig.6 : Centre-core temperature curves for cases A, B, and C

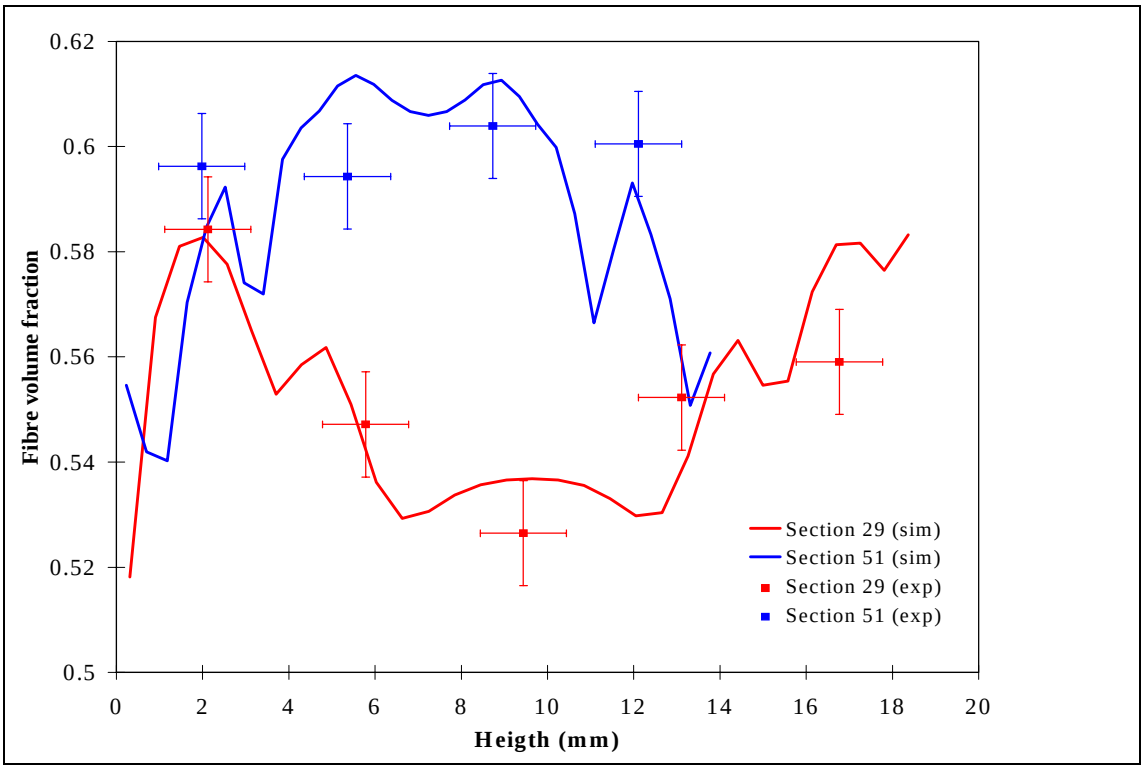

Fig.7 : Intermediate and end fibre distributions for case A

CONCLUSION

It is shown in this article that the software LAME2D, developed to simulate the compression moulding of unidirectional leaf springs, although simple in its formulation, is able to provide a quite accurate prediction of the temperature evolution and fibre distribution in the springs. The numerical tool is quick and easy to handle.
At the moment, the main weakness of the model is the impossibility to calculate the complete temperature profiles at the surface of the multiblocks regulated tools. This would lead to a much heavier model. A more complex model, taking into account transversal and end-of-ply fluxes would also allows us to reach better accuracy, but we should have difficulties to check the numerical results, as we are also limited by the experimental methods accuracy.

REFERENCES

1. Halley, P.J. and Mackay, M.E., « Chemorheology of thermosets - An overview », *Polymer Engineering and Science*, Mid-March 1996, Vol.36, N°5, pp. 593-609
2. Carman, P.C., « Fluid flow through granular beds », *Trans. Int. Chem. Eng*, 1939, Vol.15, pp. 150-166
3. Lekakou, C., et al, « Measurement techniques and effects on in-plane woven cloths in resin transfer moulding » , *Composites Part A*, 1996, Vol.27A, pp. 401-408
4. Hoareau C., « Injection sur renfort - Etude du remplissage de moule et détermination théorique de la perméabilité des tissus.», PhD Thesis, Ecole Nationale Superieure des Mines de Paris, CEMEF, 1994
5. Van der Westhuizen, J., Prieur Du Plessis, J. , « An attempt to quantify fibre bed permeability utilizing the phase average Navier Stokes equation », *Composites Part A*, 1996, Vol. 27A, pp. 263-269
6. Berdichevsky, A. L., Cai, Z., « Preform permeability predictions by self-consistent method and finite element simulation », *Polymer Composites*, April 1993, Vol.14, N°2, pp. 132-143
7. Natola, A., Charvet, T., « Simulation numérique de la thermique des outillages », STRUCOME 95, pp. 489-502